Inhibition of efflorescence in mixed organic–inorganic particles at temperatures less than 250 K

A. Bodsworth,[a] B. Zobrist[b] and A. K. Bertram*[a]

Received 14th May 2010, Accepted 12th July 2010
DOI: 10.1039/c0cp00572j

It is now well recognized that mixed organic–inorganic particles are abundant in the atmosphere. While there have been numerous studies of efflorescence of mixed organic–inorganic particles close to 293 K, there are only a few at temperatures less than 273 K. Understanding the efflorescence properties of these particles at temperatures less than 273 K could be especially important for predicting ice nucleation in the upper troposphere. We studied the efflorescence properties of mixed citric acid–ammonium sulfate particles as a function of temperature to better understand the efflorescence properties of mixed organic–inorganic particles in the middle and upper troposphere. Our data for 293 K illustrate that the addition of citric acid decreases the ERH of ammonium sulfate, which is consistent with the trends observed with other systems containing highly oxygenated organic compounds. At low temperatures the trend is qualitatively the same, but efflorescence can be inhibited by smaller concentrations of citric acid. For example at temperatures <250 K an organic mass/(organic mass + sulfate mass) of only 0.33 is needed to inhibit efflorescence of ammonium sulfate. In the upper troposphere the organic mass/(organic mass + sulfate mass) can often be larger than this value. As a result, particles in the upper troposphere may be more likely to remain in the liquid state than previously thought and solid ammonium sulfate may be less likely to participate in heterogeneous ice nucleation in the upper troposphere. Additional studies are required on other model organic systems.

1. Introduction

Measurements show that both organic and inorganic materials are abundant in atmospheric aerosols,[1] with the ratio of organic species to inorganic material depending on location, aerosol source and season. In addition, single particle measurements suggest that the dry organic mass fraction, organic/(organic + sulfate), in the upper troposphere ranges from 0.3 to 0.8 with more variation below 5 km. There are also abundant data from single particle measurements that show that organic and inorganic materials are often internally mixed in the same particles.[2–4] These internally mixed organic–inorganic particles can undergo a range of phase transitions including deliquescence and efflorescence.

Efflorescence occurs when an aqueous aerosol is exposed to a low relative humidity and the inorganic and/or organic components crystallize. The reverse process is deliquescence, where a crystalline particle exposed to a high relative humidity takes up water to form an aqueous droplet. Deliquescence is thought to be a thermodynamically controlled process and occurs at a higher relative humidity than efflorescence. Between the deliquescence relative humidity (DRH) and efflorescence relative humidity (ERH) is a metastable region where particles can be crystalline, partially crystalline, or aqueous droplets, depending on their history. Recent work has shown that in most cases the organic component in the mixed organic–inorganic particles will not effloresce since the concentration of any one organic species is small.[5] The inorganic component, however, can deliquesce and effloresce.

Understanding and predicting the deliquescence and efflorescence properties of mixed organic–inorganic particles may be important for several reasons. For example laboratory studies have shown that N_2O_5 hydrolysis is more efficient on aqueous deliquesced particles compared to effloresced particles.[6,7] In addition effloresced particles are smaller than the corresponding deliquesced particles and have different optical properties.[4,8] Modelling studies suggest that the hysteresis effect of sulfate can change the direct effect by as much as 16%.[9]

Recently several studies have focused on the deliquescence and efflorescence of mixed organic–inorganic particles.[5,10–24] To date, however, most of these studies have focused on temperatures around 293 K, and there has only been one study of the efflorescence properties of mixed organic–inorganic particles at temperatures less than 273 K.[25] While room temperature studies are useful for understanding the phase properties of atmospheric aerosols in the lower troposphere, information on the temperature dependence of these phase transitions are still needed for predicting the deliquescence and efflorescence properties of aerosol particles in the middle and upper troposphere. In the following we have investigated the efflorescence properties of mixed organic–inorganic particles at temperatures down to 233 K.

Low temperature ERH measurements may be especially important for predicting ice nucleation in the troposphere.

[a] *Department of Chemistry, University of British Columbia, Vancouver, British Columbia, Canada. E-mail: bertram@chem.ubc.ca.*
[b] *Institute for Atmospheric and Climate Science, ETH Zurich, Zurich, Switzerland*

Deliquesced particles (free of foreign nuclei such as mineral dust) can only form ice by homogeneous nucleation, whereas effloresced particles can potentially act as heterogeneous ice nuclei.[25–30] It has been shown that effloresced ammonium sulfate particles can act as good heterogeneous ice nuclei under certain conditions. These effloresced ammonium sulfate particles may compete with other effective ice nuclei in the atmosphere, and as a result, they could play an important role in climate and the aerosol indirect effect.[28] Closely related to the above, Jensen *et al.*[31] examined the properties of cirrus clouds at low temperatures in the tropical tropopause layer (TTL) and concluded that ice number concentrations, ice crystal size distributions and cloud extinctions were inconsistent with homogeneous nucleation. The authors suggested heterogeneous ice nucleation on effloresced ammonium sulfate particles as a possible mechanism to explain the *in situ* and remote-sensing measurements. Froyd *et al.*[32] also suggested heterogeneous ice nucleation on effloresced ammonium sulfate particles as a possible mechanism to explain the composition of residual particles from evaporated cirrus ice crystals near the TTL. This mechanism assumes that mixed organic–inorganic particles will effloresce in the TTL or upper troposphere.

There are some data that suggest that the efflorescence properties of mixed organic–inorganic particles may be different at low temperatures compared to 293 K. Studies by Mullin and Leci[33,34] more than 40 years ago have shown that the rate of nucleation in concentrated citric acid aqueous solutions decreases at temperatures less than 273 K,[33] possibly due to an increase in viscosity at lower temperatures. The rate of efflorescence of mixed organic–inorganic particles may decrease at lower temperatures due to an increase in viscosity as well. In addition recent studies have shown that aqueous organic components[35,36,37] and aqueous organic–inorganic[36] particles can form glasses under atmospherically relevant conditions.[38] The formation of glasses should limit efflorescence. On the other hand, Wise *et al.*[25] studied mixed palmitic acid–ammonium sulfate particles at temperatures down to 245 K and found that insoluble palmitic acid had little effect on the efflorescence properties of ammonium sulfate.

In the following we study the efflorescence properties of mixed citric acid–ammonium sulfate particles as a function of temperature. Citric acid (COOH–CH_2–COH(COOH)–CH_2–COOH, molar weight: 192.12 g mol^{-1}) contains three carboxyl groups (–COOH) and an alcohol group (–OH) and exists in the atmosphere in small quantities.[39] We also investigated the glass transition temperatures of mixed citric acid–ammonium sulfate solutions using a Differential Scanning Calorimeter (DSC) in order to relate efflorescence limitation to glass formation of the particles. Citric acid has recently been used as a model system to represent oxygenated organics in the atmosphere.[35,38] Also aqueous solutions of citric acid often form glasses at low temperatures.[40,41] Ammonium sulfate was chosen for these studies since it is an important inorganic species in the atmosphere. Also, for the conditions studied by Jensen *et al.* discussed above, the sulfate was fully neutralized to ammonium sulfate, which has recently been supported by single particle mass spectrometer data taken at the tropical tropopause.[32]

2. Experimental

The technique used to study efflorescence has been described in detail elsewhere.[17,19,42] A brief overview is provided here with a focus on details specific to the current experiments. The system consists of an optical microscope (using polarized light) coupled to a temperature controlled flow cell. The bottom surface of the flow cell is a hydrophobic glass slide upon which the particles of interest are deposited and observed. Relative humidity in the cell was controlled by a continuous flow of a mixture of humid and dry N_2. Typical flow rates were approximately 1.5 L min^{-1}.

Efflorescence experiments were conducted at five temperatures ranging from 293 K to 233 K. During experiments the particles were first deliquesced by exposing them to an RH close to 100%. Next the humidity was reduced to approximately 50% RH in one step and then decreased by approximately 0.1% RH per minute for the remainder of the experiments. During the experiments images were taken every 15 s by a camera coupled to the microscope. Particles ranged in size from 5–30 μm in diameter. For each particle, the efflorescence relative humidity (ERH) was considered to be the first appearance of solid in the particle, even if the particles appeared only partially crystalline.

Ammonium sulfate (Fisher, 99.8%) and citric acid (Sigma-Aldrich, 99 + %) were used as supplied. Bulk mixtures were prepared gravimetrically and dissolved in millipore filtered water (18.2 MΩ). To prepare the particles the solution was passed through a nebulizer to produce submicron particles. These particles were directed towards a hydrophobic glass slide where they coagulated into supermicron droplets.

The compositions of particles and/or solutions are typically reported in dry mole fraction citric acid. This dry mole fraction is calculated by the following equation:

$$X_{\mathrm{CA,dry}} = \frac{n_{\mathrm{CA}}}{n_{\mathrm{CA}} + n_{\mathrm{AS}}} \quad (1)$$

where $X_{\mathrm{CA,dry}}$ is the mole fraction of citric acid in a dry (containing no water) particle or solution, n_{CA} is the moles of citric acid and n_{AS} is the moles of ammonium sulfate. Keep in mind, however, that this does not imply the particles and solutions are completely dry. This nomenclature is used since it is a convenient method for representing the citric acid-to-ammonium sulfate ratio in particles and solutions.

Glass transition temperatures of different citric acid–ammonium sulfate–water solutions were performed in a commercial DSC (TA instruments Q10). In one set of experiments, the mass fractions of the total solutes (citric acid and ammonium sulfate) varied between 0.603 and 0.7916, whereas $X_{\mathrm{CA,dry}}$ stayed constant at 0.7. In the second set of experiments, the total mass fraction of solutes was kept at roughly 0.6, whereas the $X_{\mathrm{CA,dry}}$ was changed. All experiments were performed with bulk samples. Ammonium sulfate (Fluka, > 99.5%) and citric acid (Fluka, > 99.5%) were used as supplied. The glass transition temperatures were determined as the onset of the heat signal in the heating cycle, and have accuracy in the absolute temperature of ±0.9 K.[36]

3. Results

3.1 ERH of pure ammonium sulfate ($X_{CA,dry}$ = 0.0) *vs.* temperature

Prior to studying mixed organic–inorganic particles, we studied the efflorescence properties of pure ammonium sulfate particles as a function of temperature. This provided a reference point for the mixed organic–inorganic particles, as well as a way to validate our system for low temperature studies.

Measurements shown in Fig. 1 (solid symbols) are our results for pure ammonium sulfate particles. The solid symbols refer to the average RH. Since efflorescence is a stochastic process, all the particles did not effloresce at the same RH even for the same temperature. The error bars represent a combination of the range over which 95% of the particles efflorescence (2σ) as well as the uncertainty from measuring the relative humidity. The data suggest that efflorescence of ammonium sulfate between 293 K and 233 K is relatively insensitive to temperature; this trend follows closely the temperature trend for deliquescence of ammonium sulfate, which only varies by roughly 4% RH over 50 K.[43] Also included in Fig. 1 are results from other groups that have studied the same temperature range. The previous studies include a range of different techniques including an electrodynamic balance (EDB)[44] where a particle is suspended in an electric field and aerosol flow tubes[45,46] where the particles are suspended in a gas flow. The good agreement between our measurements and previous measurements where particles were not in contact with a surface suggests that the hydrophobic support in our experiments do not significantly affect our efflorescence results, a conclusion that is consistent with previous studies from our laboratory[18,19,47] and other groups.[21,48]

3.2 ERH of mixed ammonium sulfate–citric acid particles at room temperature

Shown in Fig. 2 are our results for mixed ammonium sulfate–citric acid particles at room temperature. Similar to Fig. 1, the symbols represent the average efflorescence relative humidity. For experiments where more than 20 particles were observed at a given concentration, the error bar corresponds to $\pm 2\sigma$ for the results as well as the uncertainty of the hygrometer ($\sim$1.1%). In cases where less than 20 nucleation events were observed the error bars correspond to $\pm$7.8%. This is a conservative estimate based on the maximum 2σ observed in our experiments where more than 20 nucleation events were observed. Our results illustrate that the addition of citric acid slowly decreases the ERH of ammonium sulfate in the particles. At 0.25 mole fraction the decrease is approximately 10% RH. At 0.3 mole fraction the particles did not effloresce at all, even when exposed to our system's minimum (RH < 1%) for longer than an hour. Also shown in Fig. 2 are results from other groups who studied the efflorescence of mixed citric acid–ammonium sulfate particles at room temperature. Choi and Chan used an EDB to study a citric acid mole fraction of $\sim$0.59. In these studies they did not observe crystallization, consistent with our measurements.[16] Zardini *et al.* used both an EDB and hygroscopicity tandem differential mobility analyzer (HTDMA) to study efflorescence. All the data from Zardini *et al.* are in excellent agreement with our data except at $X_{CA,dry}$ = 0.2, where they see a slightly higher ERH than observed in our studies. When comparing the data sets a relevant parameter is the change in ERH when going from pure ammonium sulfate to $X_{CA,dry}$ = 0.2. Zardini observed a decrease in ERH between 0–3%; whereas, we observed a decrease between 2–15%. Considering the uncertainties in the measurements the differences between data sets appear to be relatively small.

The general trend illustrated in Fig. 2 (decrease in efflorescence with addition of organic compounds) for citric acid–ammonium sulfate is consistent with the trends observed with systems

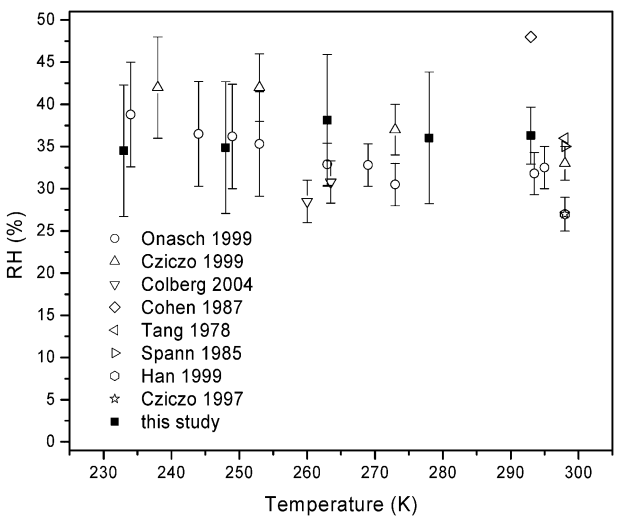

Fig. 1 Measurements of the efflorescence of pure ammonium sulfate as a function of temperature. Filled squares are this study, unfilled symbols represent ref. 44–46, 49, 63–66.

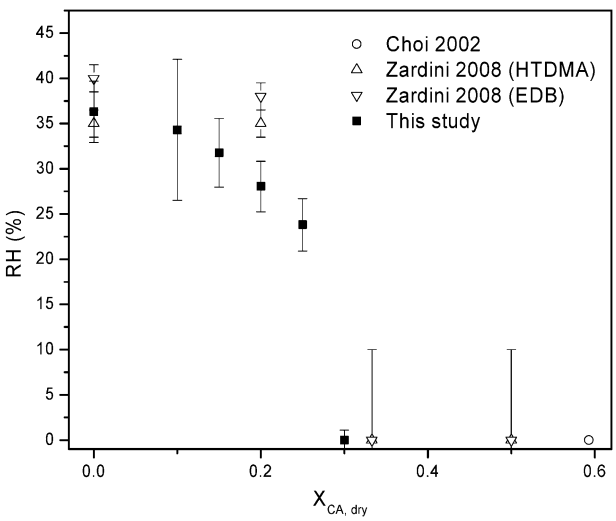

Fig. 2 Efflorescence of citric acid–ammonium sulfate particles at room temperature. Filled squares represent this study, unfilled circles represent Choi and Chan,[16] unfilled triangles are Zardini *et al.*[20] For compositions of 0.33 and 0.5 Zardini *et al.*[20] did not observe efflorescence at RH values greater than or equal to an RH of 10%. Experiments were not carried out at RH values less than 10%, and the symbols and error bars at these compositions are used to indicate this fact.

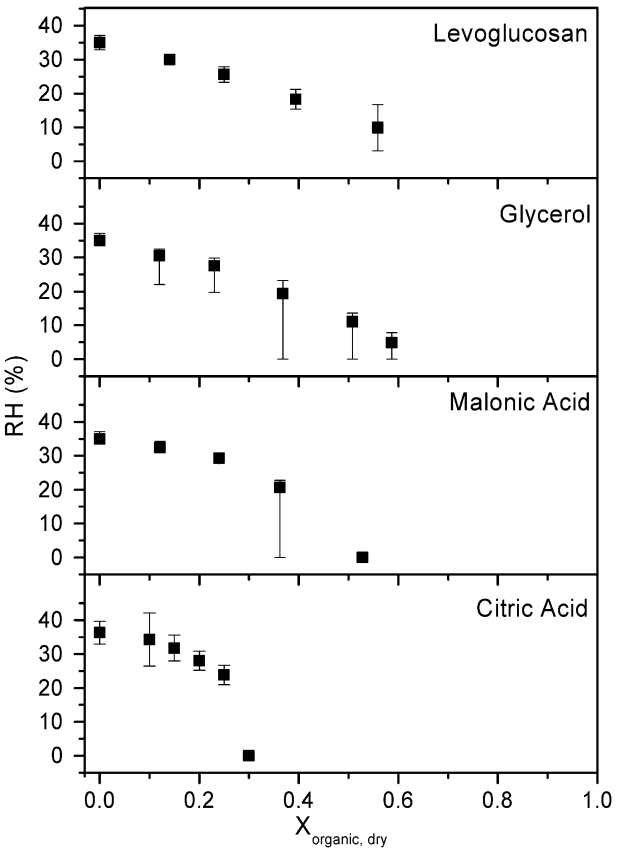

Fig. 3 Room temperature comparison between citric acid (this study) and several organics studied previously in our laboratory.[19]

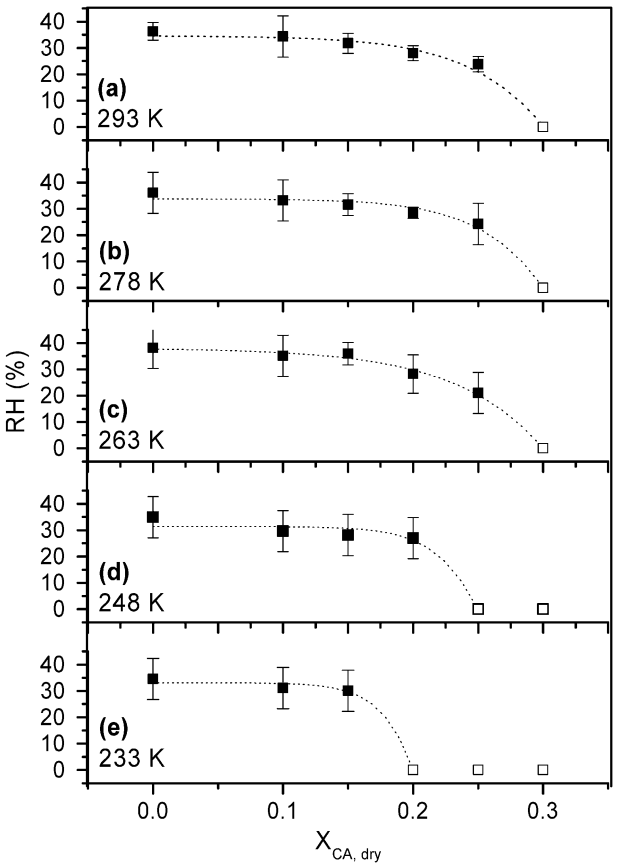

Fig. 4 Efflorescence data for different dry organic mole fractions of citric acid–ammonium sulfate particles. Different panels represent different temperatures, solid points represent observed efflorescence events and unfilled points are non-effloresing mixtures. The dashed line is included to help guide the eye.

containing other highly oxygenated organic species. To illustrate this point, we compare in Fig. 3 the results from our citric acid studies with previous measurements from our group which utilized a similar apparatus. Included in the figure are results for malonic acid, glycerol and levoglucosan.[19] The results illustrate that all systems have a similar trend, but there are significant quantitative differences between the systems. For example at a mole fraction of 0.3 the citric acid system does not effloresce whereas the malonic acid system effloresces at roughly 20.7% RH.

The differences between systems shown in Fig. 4 may be explained by classical nucleation theory. In our experiments the efflorescence relative humidity is expected to be limited by the rate of homogeneous nucleation of ammonium sulfate in the particles since the rate of crystal growth is almost instantaneous based on observations of particles during efflorescence events. According to classical nucleation theory the rate of homogeneous nucleation of crystalline ammonium sulfate in the particles can be described by the following equation, where the nucleation rate, J, is the number of nuclei formed for a unit volume and time.[50]

$$J = A \exp\left[-\frac{16\pi\gamma^3 v^2}{3k^3T^3(\ln S)^2} + \frac{\Delta G'}{kT}\right] \qquad (2)$$

where A is a pre-exponential factor, k is Boltzmann's constant, v is the molecular volume of ammonium sulfate, T is temperature, S is the supersaturation of crystalline ammonium sulfate, γ is the interfacial energy between the embryo and the surrounding liquid and $\Delta G'$ is a molecular rearrangement term (which is strongly correlated to viscosity). As discussed previously, one possible explanation for the variation in efflorescence from system to system is that γ varies significantly from system to system. This would lead to considerably different nucleation rates at a similar relative humidity since the surface tension is cubed. Another possibility is that at low RH, viscosity may become significant and vary from system to system at high mole fractions of organics. In this case, viscosity can limit the nucleation rate (through $\Delta G'$). A final possibility is that the degree of supersaturation at a given RH varies significantly from system to system due to non-ideal behavior.

3.3 ERH as a function of temperature

Fig. 4 shows the efflorescence results for the five temperatures studied. Qualitatively, the trend observed at lower temperatures remains the same, where increasing amounts of organic cause a slight reduction in ERH followed by a complete inhibition. However, at 248 K and 233 K the efflorescence is inhibited at lower mole fractions, at 0.25 and 0.2, respectively. This suggests that at low temperatures efflorescence can be inhibited by smaller concentrations of citric acid.

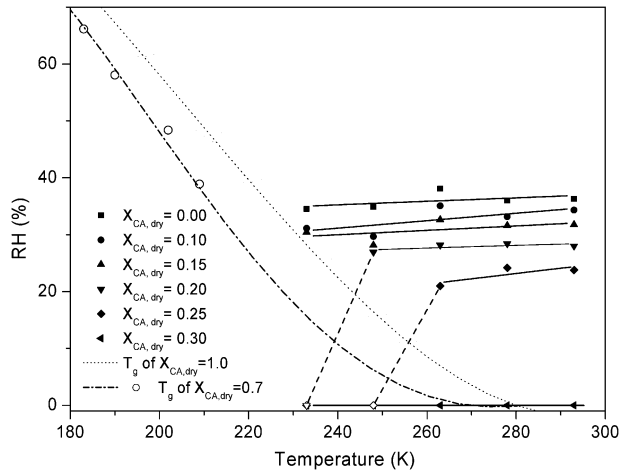

Fig. 5 Efflorescence data from this study combined with calculated glass transition data (see text for further details). The dotted line represents the T_g of a binary mixture of water and citric acid ($X_{CA,dry}$ = 1.0). The dash-dot line and open symbols correspond to ternary mixtures with $X_{CA,dry}$ = 0.7.

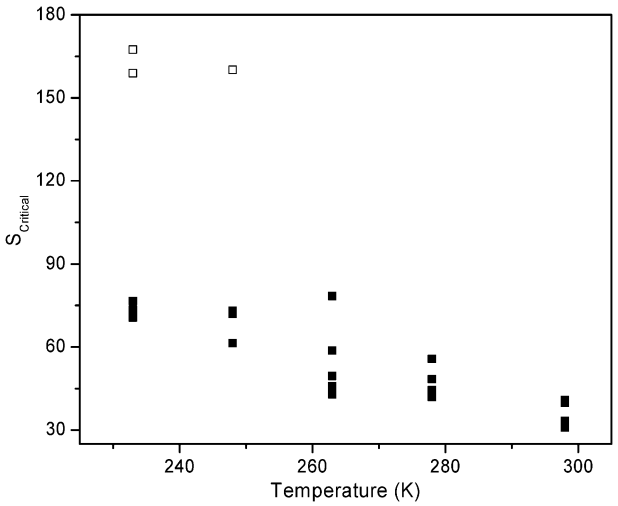

Fig. 6 The supersaturation required to induce efflorescence, $S_{critical}$, observed in our experiments. The solid points correspond to observed efflorescence events while unfilled points represent the lower limit associated with non-efflorescing mixtures.

Fig. 5 shows the same data as Fig. 4, replotted in RH–temperature space. This figure more clearly illustrates that the efflorescence for $X_{CA,dry}$ = 0.0, 0.1 and 0.15 is relatively insensitive to temperature. A linear fit for these three data sets shows slopes between 0.03 and 0.07% RH per Kelvin. Fig. 5 also illustrates that at $X_{CA,dry}$ = 0.2 and 0.25 the ERH is a strong function of temperature, with a sudden change in ERH at 233 K and 248 K for $X_{CA,dry}$ = 0.2 and 0.25 respectively. Similar to Fig. 4, this shows that at low temperatures (<250 K) and high organic concentrations ($X_{CA,dry}$ = 0.2 and 0.25) efflorescence appears to be inhibited.

Recently in a notable set of experiments Wise *et al.*[25] studied the efflorescence properties of ammonium sulfate particles coated with palmitic acid down to approximately 245 K. These authors observed efflorescence at approximately 35% RH for the entire temperature range studied and noted that the organic coating had little effect on the efflorescence of ammonium sulfate. One likely reason for the difference between our results and the results by Wise *et al.* is the properties of the organic material studied. Palmitic acid is insoluble in water. On the other hand, citric acid is water soluble and does not crystallize under the conditions we explored.

3.4 Explanation of temperature dependence

Again, the temperature dependence of the ERH may be rationalized with classical nucleation theory and eqn (2). One possible explanation for the efflorescence inhibition illustrated in Fig. 4 and 5 is that the particles which were rich in organics (0.20 and 0.25 mole fractions) and at lower temperatures do not reach a large supersaturation with respect to ammonium sulfate ($S_{(NH_4)_2SO_4}$), possibly due to non-ideal solution behaviour. As a result the driving force for efflorescence (*i.e.* S variable in eqn (2)) is smaller at the lower temperatures and in the most concentrated particles. To explore this we calculated the $S_{(NH_4)_2SO_4}$ reached in all experiments where efflorescence was observed using the e-AIM model.[51] These results are represented by solid symbols in Fig. 6. Although e-AIM assumes that ion–organic component interactions are minor, it has been used to represent this system in 1 : 1 mole ratio previously with some success.[52] In general, supersaturations with respect to ammonium sulfate ranged from 30 to approximately 75. Next we calculated lower limits to the $S_{(NH_4)_2SO_4}$ reached in the experiments where efflorescence was not observed. The results from these calculations are represented by the open symbols in Fig. 6. To calculate these lower limits we used the e-AIM model and an RH of 10%. In the experiments where no efflorescence was observed $S_{(NH_4)_2SO_4}$-values greater than 150 were reached which is clearly larger than the $S_{(NH_4)_2SO_4}$-values reached in the experiments where efflorescence was observed. We conclude that low $S_{(NH_4)_2SO_4}$-values at the lowest temperatures and in particles with greater organic component loadings cannot explain our observations.[53–56]

The inhibition trend at low temperatures observed in our experiments may be related to crystallization studies in aqueous citric acid solutions carried out 40 years ago.[33] The authors argued that the decrease in nucleation events at lower temperatures was due to an increase in viscosity which would increase $\Delta G'$ in eqn (2). An increase in viscosity could also explain the observed inhibition of efflorescence of mixed ammonium sulfate–citric acid particles at the lowest temperatures in our experiments.

3.5 Possible connections with glass transition temperatures

As mentioned in the Introduction, recent work has shown that both organic particles and mixed organic–inorganic particles can form glasses at low temperatures of atmospheric relevance.[35,36] Prior to our work there have not been any reports of glass transition temperatures of citric acid–ammonium sulfate–water solutions. Below we investigated the glass transition temperatures of these solutions using a DSC and relate these values to the observed efflorescence conditions.

Shown in Fig. 7 (solid symbols) are the glass transition temperatures, T_g, we determined for mixed citric acid–ammonium sulfate–water solutions as a function of total mass fraction

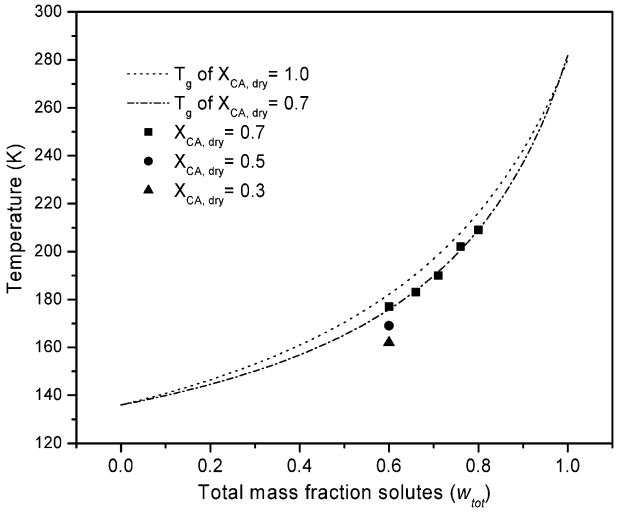

Fig. 7 Glass transition temperatures of citric acid–ammonium sulfate solutions as a function of the total mass fraction of the solutes. Squares: $X_{CA,dry} = 0.7$; circle: $X_{CA,dry} = 0.5$ and triangle: $X_{CA,dry} = 0.3$. The dash-dot line is a fit to the data for $X_{CA,dry} = 0.7$ using eqn (3). The dashed line is a parameterization of the glass transition temperatures of citric acid–water solutions taken from the literature (see the text for more details).

solutes. Each T_g is a mean value of two single measurements. Note we were unable to measure glass transition temperatures for a wider range of solute mass fractions or for different $X_{CA,dry}$-values since in these solutions either ice or ammonium sulfate crystallization was observed before reaching the glass state. The solid line through the square symbols is a parameterization of the experimental data for $X_{CA,dry} = 0.7$ using the Gordon–Taylor equation.[57] Gordon and Taylor first postulated an equation which allows computing the glass transition temperature of aqueous solutions, T_g, as a function of the mass fraction of the solute, w_2:

$$T_g(w) = \frac{w_1 T_{g1} + \frac{1}{k} w_2 T_{g2}}{w_1 + \frac{1}{k} w_2}, \qquad (3)$$

where w_1 is the mass fraction of water, T_{g1} and T_{g2} are the glass transition temperatures of pure water and of the solute, respectively. For $X_{CA,dry}$ values of 0.7 we fit the experimental data to this equation using T_{g1} as 136 K.[58,59] The parameters from the fit are $T_{g2} = 273.6$ K and $k = 4.383$.

Also shown in Fig. 7 (dashed line) is a parameterization of the glass transition temperatures of citric acid–water solutions taken from the literature.[41] The citric acid–water data correspond to $X_{CA,dry} = 1.0$.

In Fig. 5, we have plotted the glass transition temperatures for $X_{CA,dry} = 1.0$ and 0.7 from Fig. 7 in RH–temperature space. For both the binary and ternary systems we used the extended-AIM model to relate the composition of the mixtures to RH. Note that the T_g-values for $X_{CA,dry} = 0.5$ and 0.3 shown in Fig. 7 have not been included in Fig. 5, since the extended-AIM model is limited to temperatures above 180 K. The T_g-values for $X_{CA,dry} = 1.0$ and 0.7 shown in Fig. 5 should be upper limits to the T_g-values for $X_{CA,dry} = 0.0$ to 0.3 (which is the composition range used in the efflorescence experiments). This is because the addition of ammonium sulfate decreases the T_g of the system as shown in Fig. 5 and 7. As a result the T_g-values shown in Fig. 5 are insufficient to argue that glass formation is responsible for the inhibition of efflorescence observed in our studies with $X_{CA,dry} = 0.0$ to 0.3. Nevertheless it is interesting to note that the glass transition temperatures shown are very close to the temperatures and RH values where we observed inhibition of efflorescence.

3.6 Atmospheric implications

This study has shown that relatively small quantities of citric acid can completely suppress efflorescence of ammonium sulfate at low temperatures. For example, Fig. 4 suggests that at temperatures below 233 K, mixed citric acid–ammonium sulfate particles will not effloresce if $X_{CA,dry} \geq 0.2$. This corresponds to a dry organic mass fraction (organic mass/(organic mass + sulfate mass)) of ≥ 0.33. Recent field studies using single particle mass spectrometry suggests that the dry organic mass fraction in the upper troposphere is 0.3 to 0.8.[60] If we assume that 60% to 90% of the total organics mass is water soluble[61,62] in the free troposphere, we obtained a water soluble organic mass fraction (organic mass/(organic mass + sulfate mass)) of 0.18 to 0.72. It is interesting to note that the dry organic mass fraction where we see inhibition of efflorescence (≥ 0.33) is within the composition range of importance in the atmosphere (0.18 to 0.72). The current study is only a first step toward understanding the ERH properties of mixed organic–inorganic particles in the middle and upper troposphere. Additional studies are required on other model organic systems. Nevertheless our data do point out that the efflorescence properties of mixed organic–inorganic particles can be different at low temperatures compared to room temperature and only small amounts of water soluble organic material may be needed to inhibit efflorescence of ammonium sulfate. As a result, particles in the upper troposphere may be more likely to remain in the liquid state than previously thought and solid ammonium sulfate may be less likely to participate in heterogeneous ice nucleation in the upper troposphere.

As mentioned above, we see a different trend to that observed by Wise *et al.*[25] who used particles composed of palmitic acid and ammonium sulfate. The palmitic acid results may be more relevant to conditions where the organics are insoluble in water. Our citric acid results may be more relevant for conditions where the organics are water soluble and do not effloresce (*i.e.* remain in the liquid state or glass state) for atmospheric conditions.

4. Conclusions

We studied the efflorescence properties of mixed citric acid–ammonium sulfate particles as a function of temperature to better understand the efflorescence properties of mixed organic–inorganic particles in the middle and upper troposphere. Our data for 293 K illustrate that the addition of citric acid decreases the ERH of ammonium sulfate in the particles, which is consistent with the trends observed with other highly oxygenated organic systems. At low temperatures the trend is qualitatively the same, but at these low temperatures efflorescence can be inhibited by smaller concentrations of citric acid.

In other words, this study shows that at low temperatures relatively small quantities of citric acid can completely suppress the efflorescence of ammonium sulfate. For example at temperatures <250 K a citric acid dry mole fraction of only 0.2 is needed to inhibit efflorescence ammonium sulfate in the particles. This corresponds to a dry organic mass fraction of only 0.33. In the upper troposphere the dry mass fraction of water soluble organics is often larger than this value. Additional studies are required on other model organic systems. Nevertheless our data do point out that the efflorescence properties of mixed organic–inorganic particles can be different at low temperatures compared to room temperature and only small amounts of water soluble organic material may be needed to inhibit efflorescence of ammonium sulfate. As a result, particles in the upper troposphere may be more likely to remain in the liquid state than previously thought and solid ammonium sulfate may be less likely to participate in heterogeneous ice nucleation in the upper troposphere.

Acknowledgements

This research was supported by the Canadian Foundation for Climate and Atmospheric Science (CFCAS), the National Sciences and Engineering Research Council of Canada (NSERC), and the Canada Research Chair Program. The authors thank U.K. Krieger for helpful discussions regarding the project.

References

1 Q. Zhang and J. L. Jimenez, *et al.*, *Geophys. Res. Lett.*, 2007, **34**(13), DOI: 10.1029/2007GL029979.
2 D. M. Murphy and D. S. Thomson, *et al.*, *Science*, 1998, **282**(5394), 1664–1669.
3 D. M. Murphy and D. J. Cziczo, *et al.*, *J. Geophys. Res., [Atmos.]*, 2006, **111**(D23), DOI: 10.1029/2006JD007340.
4 G. Buzorius and A. Zelenyuk, *et al.*, *Geophys. Res. Lett.*, 2002, **29**(20), DOI: 10.1029/2001GL014221.
5 C. Marcolli and B. P. Luo, *et al.*, *J. Phys. Chem. A*, 2004, **108**(12), 2216–2224.
6 M. Hallquist and D. J. Stewart, *et al.*, *Phys. Chem. Chem. Phys.*, 2003, **5**(16), 3453–3463.
7 J. A. Thornton and C. F. Braban, *et al.*, *Phys. Chem. Chem. Phys.*, 2003, **5**(20), 4593–4603.
8 S. T. Martin and H. M. Hung, *et al.*, *Atmos. Chem. Phys.*, 2004, **4**, 183–214.
9 J. Wang and A. A. Hoffmann, *et al.*, *J. Geophys. Res., [Atmos.]*, 2008, **113**(D11), DOI: 10.1029/2007JD009367.
10 A. Alshawa and O. Dopfer, *et al.*, *J. Phys. Chem. A*, 2009, **113**(26), 7678–7686.
11 A. Zelenyuk and D. Imre, *et al.*, *J. Aerosol Sci.*, 2007, **38**(9), 903–923.
12 E. Woods and H. S. Kim, *et al.*, *J. Phys. Chem. A*, 2007, **111**(43), 11013–11020.
13 J. M. Lightstone and T. B. Onasch, *et al.*, *J. Phys. Chem. A*, 2000, **104**(41), 9337–9346.
14 S. D. Brooks and R. M. Garland, *et al.*, *J. Geophys. Res., [Atmos.]*, 2003, **108**(D15), DOI: 10.1029/2002JD003204.
15 C. F. Braban and J. P. D. Abbatt, *Atmos. Chem. Phys.*, 2004, **4**, 1451–1459.
16 M. Y. Choi and C. K. Chan, *Environ. Sci. Technol.*, 2002, **36**(11), 2422–2428.
17 A. Pant and A. Fok, *et al.*, *Geophys. Res. Lett.*, 2004, **31**, DOI: 10.1029/2004GL020025.
18 M. T. Parsons and J. L. Riffell, *et al.*, *J. Phys. Chem. A*, 2006, **110**(26), 8108–8115.
19 M. T. Parsons and D. A. Knopf, *et al.*, *J. Phys. Chem. A*, 2004, **108**(52), 11600–11608.
20 A. A. Zardini and S. Sjogren, *et al.*, *Atmos. Chem. Phys.*, 2008, **8**(18), 5589–5601.
21 M. C. Yeung and A. K. Y. Lee, *et al.*, *Aerosol Sci. Technol.*, 2009, **43**(5), 387–399.
22 S. Takahama and R. K. Pathak, *et al.*, *Environ. Sci. Technol.*, 2007, **41**(7), 2289–2295.
23 S. D. Brooks and P. J. DeMott, *et al.*, *Atmos. Environ.*, 2004, **38**(13), 1859–1868.
24 C. L. Badger and I. George, *et al.*, *Atmos. Chem. Phys.*, 2006, **6**, 755–768.
25 M. E. Wise and K. J. Baustian, *et al.*, *Proc. Natl. Acad. Sci. U. S. A.*, 2010, **107**(15), 6693–6698.
26 B. Zuberi and A. K. Bertram, *et al.*, *J. Phys. Chem. A*, 2001, **105**(26), 6458–6464.
27 J. E. Shilling and T. J. Fortin, *et al.*, *J. Geophys. Res., [Atmos.]*, 2006, **111**(D12), DOI: 10.1029/2005JD006664.
28 J. P. D. Abbatt and S. Benz, *et al.*, *Science*, 2006, **313**(5794), 1770–1773.
29 M. E. Wise and R. M. Garland, *et al.*, *J. Geophys. Res., [Atmos.]*, 2004, **109**(D19), DOI: 10.1029/2003JD004313.
30 M. E. Wise and K. J. Baustian, *et al.*, *Atmos. Chem. Phys.*, 2009, **9**(5), 1639–1646.
31 E. J. Jensen and L. Pfister, *et al.* Ice nucleation and cloud microphysical properties in tropical tropopause layer cirrus, *Atmos. Chem. Phys.*, 2010, **10**(3), 1369–1384.
32 K. D. Froyd and D. M. Murphy, *et al.*, *Atmos. Chem. Phys.*, 2010, **10**(1), 209–218.
33 J. W. Mullin and C. L. Leci, *J. Cryst. Growth*, 1969, **5**(1), 75–76.
34 J. W. Mullin and C. L. Leci, *Philos. Mag*, 1969, **19**(161), 1075–1077.
35 B. J. Murray, *Atmos. Chem. Phys.*, 2008, **8**(17), 5423–5433.
36 B. Zobrist and C. Marcolli, *et al.*, *Atmos. Chem. Phys.*, 2008, **8**(17), 5221–5244.
37 E. Mikhailov, S. Vlasenko, S. T. Martin, T. Koop and U. Poschl, *Atmos. Chem. Phys.*, 2009, **9**, 9491–9522.
38 B. J. Murray and T. W. Wilson, *et al.*, *Nat. Geosci.*, 2010, **3**(4), 233–237.
39 P. Saxena and L. M. Hildemann, *J. Atmos. Chem.*, 1996, **24**(1), 57–109.
40 E. Maltini and M. Anese, *et al.*, *CryoLetters*, 1997, **18**(5), 263–268.
41 D. Lienhard, B. Zobrist, *et al.*, in preparation.
42 A. Pant and M. T. Parsons, *et al.*, *J. Phys. Chem. A*, 2006, **110**(28), 8701–8709.
43 I. N. Tang and H. R. Munkelwitz, *Atmos. Environ., Part A*, 1993, **27**(4), 467–473.
44 C. A. Colberg and U. K. Krieger, *et al.*, *J. Phys. Chem. A*, 2004, **108**(14), 2700–2709.
45 D. J. Cziczo and J. P. D. Abbatt, *J. Geophys. Res., [Atmos.]*, 1999, **104**(D11), 13781–13790.
46 T. B. Onasch and R. L. Siefert, *et al.*, *J. Geophys. Res.*, 1999, **104**, DOI: 10.1029/1999JD900384.
47 M. T. Parsons and J. Mak, *et al.*, *J. Geophys. Res., [Atmos.]*, 2004, **109**(D6), D06212.
48 T. Koop and A. Kapilashrami, *et al.*, *J. Geophys. Res., [Atmos.]*, 2000, **105**(D21), 26393–26402.
49 M. D. Cohen, R. C. Flanagan and J. H. Seinfeld, *J. Phys. Chem.*, 1987, **91**, 4583–4590.
50 J. W. Mullin, *Crystallization*, Elsevier Ltd., 2001.
51 S. L. Clegg, P. Brimblecombe, *et al.*, (e-AIM). Extended AIM Aerosol Thermodynamics Model, http://www.aim.env.uea.ac.uk/aim/aim.php.
52 C. H. Tong and S. L. Clegg, *et al.*, *Atmos. Environ.*, 2008, **42**(21), 5459–5482.
53 S. L. Clegg and J. H. Seinfeld, *J. Phys. Chem. A*, 2006, **110**(17), 5718–5734.
54 S. L. Clegg and J. H. Seinfeld, *et al.*, *J. Aerosol Sci.*, 2001, **32**(6), 713–738.
55 S. L. Clegg and J. H. Seinfeld, *J. Phys. Chem. A*, 2006, **110**(17), 5692–5717.
56 C. Peng and M. N. Chan, *et al.*, *Environ. Sci. Technol.*, 2001, **35**(22), 4495–4501.

57 M. Gordon and J. S. Taylor, *J. Appl. Chem.*, 1952, **2**(9), 493–500.
58 I. Kohl and L. Bachmann, *et al.*, *Phys. Chem. Chem. Phys.*, 2005, **7**(17), 3210–3220.
59 G. P. Johari and A. Hallbrucker, *et al.*, *Nature*, 1987, **330**(6148), 552–553.
60 K. D. Froyd and D. M. Murphy, *et al.*, *Atmos. Chem. Phys.*, 2009, **9**(13), 4363–4385.
61 S. F. Maria and L. M. Russell, *et al.*, *Atmos. Environ.*, 2002, **36**(33), 5185–5196.
62 Z. Krivacsy and A. Gelencser, *et al.*, *J. Atmos. Chem.*, 2001, **39**(3), 235–259.
63 I. N. Tang and H. R. Munkelwitz, *et al.*, *J. Aerosol Sci.*, 1978, **9**(6), 505–511.
64 J. F. Spann and C. B. Richardson, *Atmos. Environ.*, 1985, **19**(5), 819–825.
65 J. H. Han and S. T. Martin, *J. Geophys. Res., [Atmos.]*, 1999, **104**(D3), 3543–3553.
66 D. J. Cziczo and J. B. Nowak, *et al.*, *J. Geophys. Res., [Atmos.]*, 1997, **102**(D15), 18843–18850.

